

ARIES: Aerial Reconnaissance Instrumental Electronics System

Marissa Van Luvender^{*}, Kane Cheung[†], Hao Lam[‡], Enzo Casa[§], Matt Scott[¶], Bidho Embaie[#],
California Polytechnic University Pomona, Pomona, CA, 92504

Abstract-California Polytechnic University Pomona has developed ARIES UAV for the Association of Unmanned Aerial Vehicles (AUVSI) 2005 student competition. The Aerial Reconnaissance Instrumental Electronics System (ARIES) was developed by integrating several off-the-shelf electronics in order to achieve autonomous flight and successfully complete reconnaissance and surveillance missions using a Senior Telemaster Aircraft. A stability analysis was first completed using feedback control loops which were analyzed using MATLAB. The aircraft was flight tested to find experimental gains for the Micropilot. The Micropilot uses a Proportional-Integral-Derivative controller to stabilize aircraft response. The subsystems used to develop ARIES included: a Micropilot 2028g, a communications subsystem, an imagery subsystem, and power subsystem. The purpose of this paper is to describe the results of the stability analysis, the aircraft software and hardware subsystems, and how the subsystems interact to accomplish reconnaissance and surveillance missions.

Nomenclature

A	amplitude of oscillation
a	cylinder diameter
C_p	pressure coefficient
C_x	force coefficient in the x direction
C_y	force coefficient in the y direction
c	chord
dt	time step
F_x	X component of the resultant pressure force acting on the vehicle
F_y	Y component of the resultant pressure force acting on the vehicle
f, g	generic functions
h	height
i	time index during navigation
j	waypoint index
K	trailing-edge (TE) nondimensional angular deflection rate

^{*} Student, Aerospace Engineering Department, mvanluvender@csupomona.edu, AIAA Student Member.

[†] Student, Electrical Engineering Department, Kane.Cheung@gmail.com

[‡] Student, Aerospace Engineering Department, hhlam@csupomona.edu, AIAA Student Member.

[§] Student, Aerospace Engineering Department, efcasa@csupomona.edu.

[¶] Student, Aerospace Engineering Department, mtscott@csupomona.edu, AIAA Student Member.

[#] Student, Aerospace Engineering Department, btembaie@csupomona.edu.

L_p	rolling moment due to roll rate
L_r	rolling moment due to yaw rate
$L_{\delta a}$	rolling moment due to aileron deflection
L_{β}	rolling moment due to sideslip
$L_{\delta r}$	rolling moment due to rudder deflection
M_q	pitching moment due to pitch rate
M_u	pitching moment due to velocity in axial direction
M_w	pitching moment due to vertical velocity
$M_{w \dot{}}$	pitching moment due to vertical acceleration
M_{α}	pitching moment due to angle of attack
$M_{\alpha \dot{}}$	pitching moment due to change in angle of attack
$M_{\delta e}$	pitching moment due to elevator deflection
N_p	yawing moment due to roll rate
N_r	yawing moment due to side slip
$N_{\delta a}$	yawing moment due to aileron deflection
$N_{\delta r}$	yawing moment due to rudder deflection
$N_{1/2p}$	number of cycles for aircraft to stabilize in phugoid mode
$N_{1/2sp}$	number of cycles for aircraft to stabilize in short period mode
$t_{1/2 p}$	time for oscillation amplitude to decrease to half of initial amplitude in phugoid mode
$t_{1/2 sp}$	time for oscillation amplitude to decrease to half of initial amplitude in short period mode
T_{spiral}	time for spiral mode to decrease to half
X_u	axial force due to axial velocity
X_w	axial force due to vertical velocity
Y_{β}	side force due to sideslip
Y_p	side force due to roll rate
Y_r	side force due to yaw rate
$Y_{\delta a}$	side force due to aileron deflection
$Y_{\delta r}$	side force due to rudder deflection
Z_q	side force due to pitch rate
Z_u	normal force due to axial velocity
Z_w	normal force due to vertical velocity
$Z_{w \dot{}}$	normal force due to vertical acceleration
Z_{α}	normal force due to angle of attack
$Z_{\alpha \dot{}}$	normal force due to change in angle of attack
$Z_{\delta e}$	normal force due to elevator deflection
τ_{roll}	roll time constant
ω_{nDR}	dutch roll frequency
ω_{nsp}	short period frequency
ω_{np}	phugoid frequency
ζ_{sp}	phugoid damping ratio
ζ_{sp}	short period damping ratio
ζ_{DR}	dutch roll mode damping ratio

Table of Contents

I. Introduction

II. Aircraft Specifications

III. Stability Analysis

IV. Software Systems

V. Hardware Systems

Acknowledgements

References

I. Introduction

Aircraft have had increasingly important roles over the past century. The advancement in aircraft technology has determined the outcome of wars, our society, and the way of life. Due to the advancement in electronics, microprocessors, and sensory systems, autonomous control systems have become the way of the future. Autonomous systems reduce loss of human life and the low cost of these types of aircrafts have become increasingly desirable for both commercial and military use in flight, ground, and water vehicle and weapon applications.

In this paper, ARIES development, stability analysis, software systems, and hardware systems will be discussed. ARIES is an off-the shelf single engine gas-powered, high-mounted non-swept wing aircraft, and a standard tail configuration. ARIES will consist of a wireless camera system to photograph targets within the mission zone, an uplink and downlink to communicate and transfer images, and an autonomous flight control system to allow preset mission profiles to be programmed for flight in addition to manual override and mission alterations during flight. ARIES is capable of fully autonomous flight using pre-programmed missions and GPS waypoints, real-time surveillance, and mission alteration during flight.

II. Aircraft Specifications

ARIES was constructed from a Senior Telemaster RC Aircraft. The Senior Telemaster was chosen because it is an extremely stable aircraft with large control surfaces and large load carrying capabilities. The aircraft has a wing span of 8 ft and a wing area of approximately 9.25 ft². The horizontal tail area is 2.22 ft² and the vertical tail area is 0.47 ft². The fuselage is 5.25 ft long and has a maximum diameter of 0.33 ft. A majority of the electronics are located near the center of gravity of the aircraft which is located close to the quarter chord of the wing. The aircraft is powered by a Thunder Tiger GP-61 engine and it carries a maximum of 40 ounces of Synthetic Model Engine Fuel 15% Cool Power. A detailed model of ARIES may be viewed in Figure.1. Concentration of system development was based primarily on increased stability rather than maneuverability because of contest requirements; however, some stability was sacrificed for maneuverability to handle possible gusts or turbulence during flight. In addition, other considerations to development include limiters, and sensitivity.

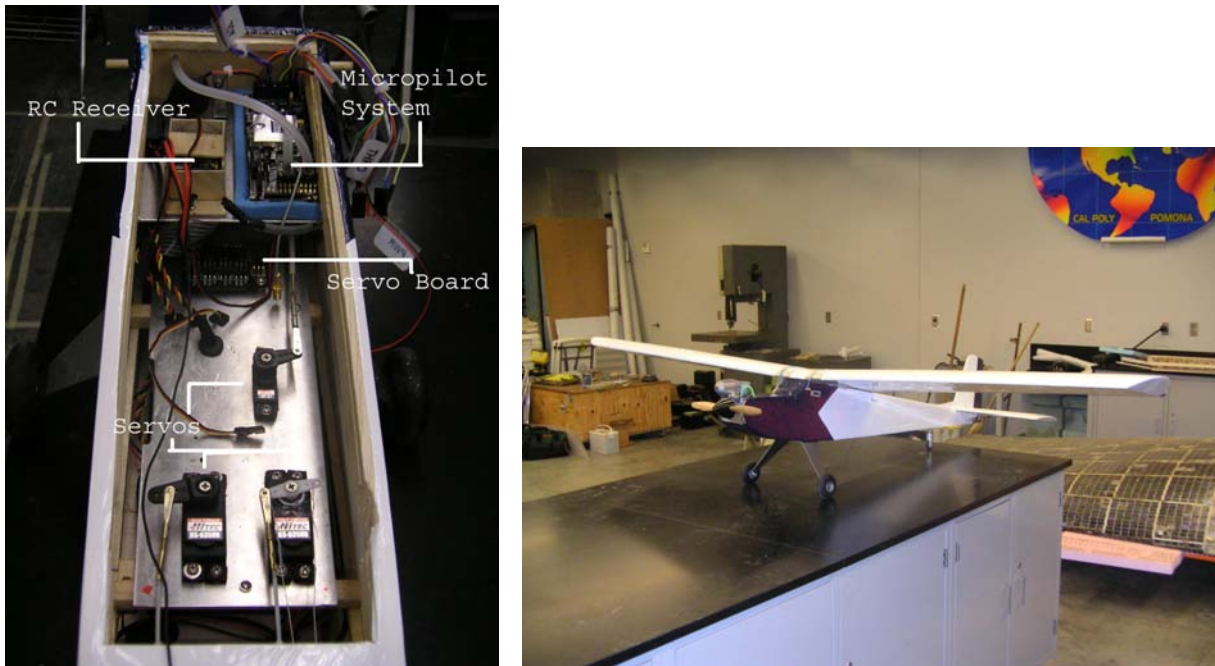


Figure 1. Detailed View of ARIES Flight System

III. Stability Analysis

To analyze the stability of ARIES, two primary control loops were generated to analyze autonomous flight during cruise. The control loops included: 1) Longitudinal control system was analyzed using an altitude sensor, pitch rate gyros, vertical gyros, elevator servos, and was altered based on required compensation networks (Figure 2), 2) Lateral control system using heading for the outer loop with two main inner loops to control yaw and roll of the aircraft. The yaw control loop theoretically consisted of components such as yaw rate gyros, and rudder servos, and was altered based on necessary compensation networks. The roll control loop theoretically contained roll rate gyros, aileron servos, and was altered based on necessary compensation networks (Figure 3). Compensation networks consisted of gains, leads, lags, or other shaping functions which were determined through root locus, and bode analysis of phugoid and short period modes by determining the aircraft characteristics such as longitudinal and lateral stability derivatives. Some minor modifications were made to manipulate the aircraft characteristics. These were compared to MIL-F-8785C Specifications in order to achieve Class 1 Level 1 characteristics.

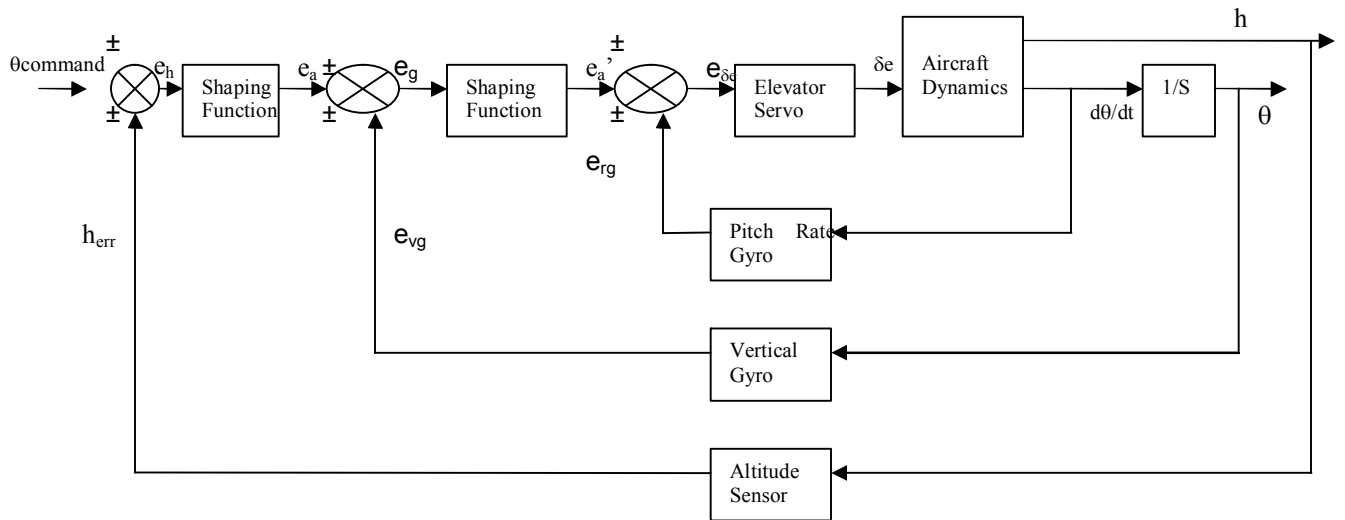


Figure 2. Longitudinal Cruise Control Loop

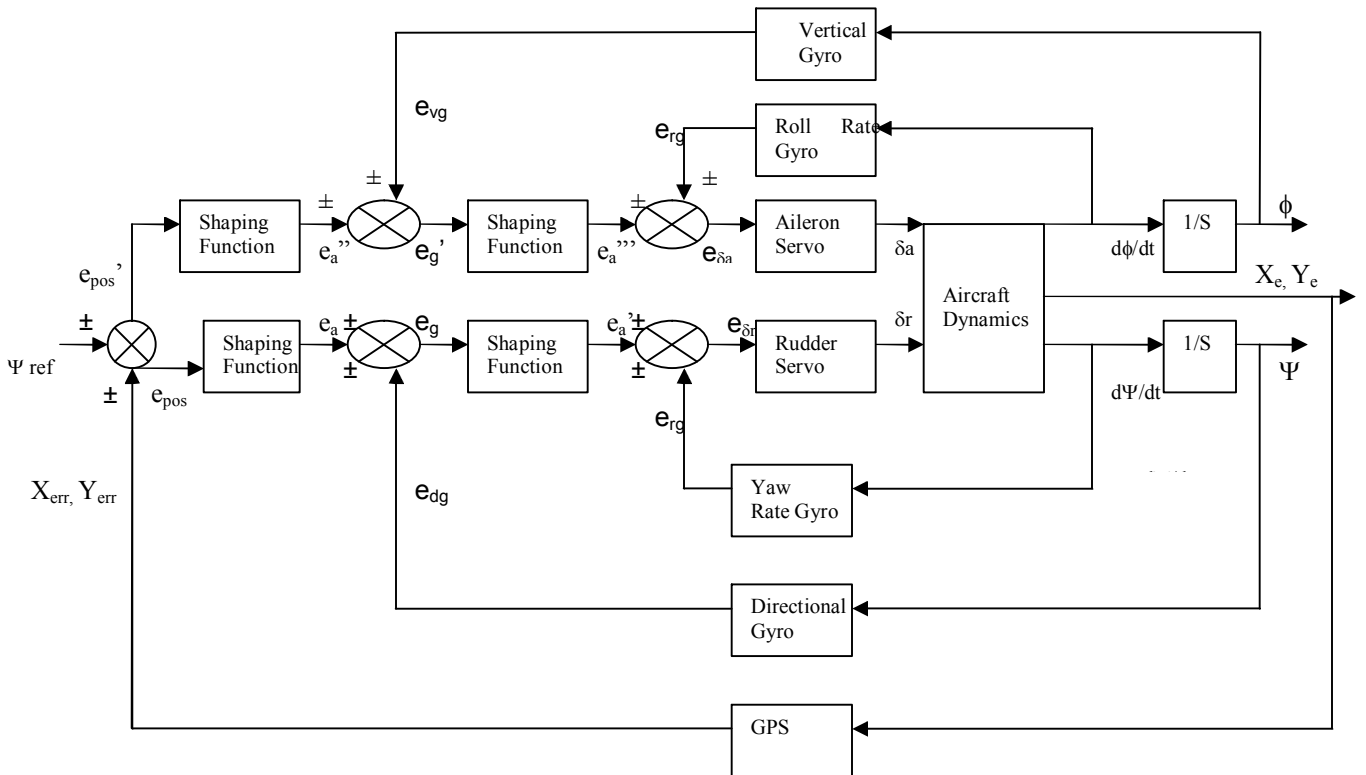


Figure 3. Lateral Cruise Control Loop

Examples of the initial root locus, bode plot, and step response may be viewed in Figures 4, 5, and 6. The root locus shown was analyzed for initial aircraft response for direction control with respect to elevator deflection.

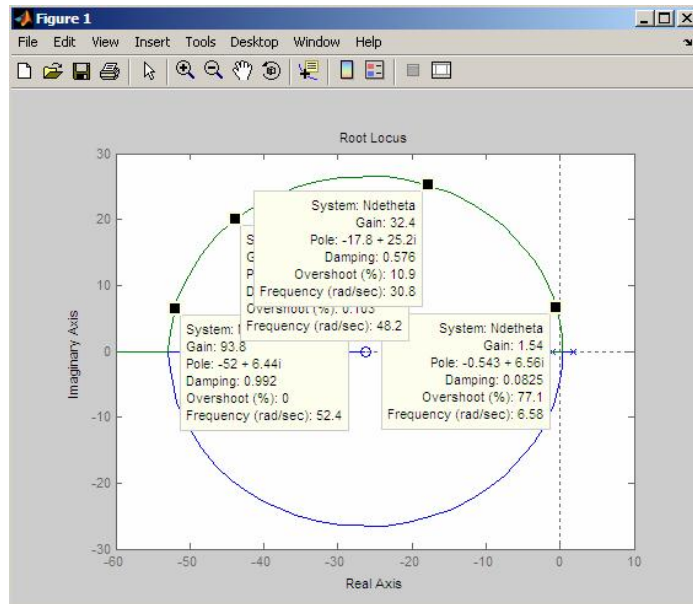


Figure 4. Open Loop Root Locus Plot for Initial Aircraft Directional Response Due to Elevator Deflection

In Figure 4, an example bode plot for the initial aircraft roll response due to rudder deflection may be viewed.

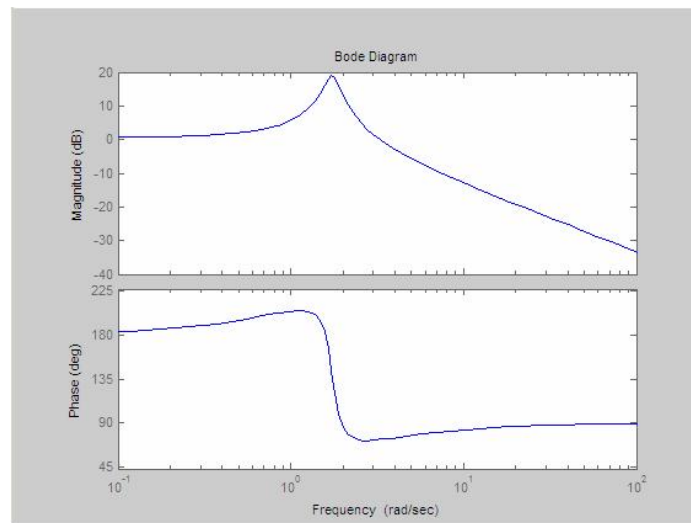


Figure 5. Bode Plot for Initial Aircraft Roll Response Due to Elevator Deflection

In Figure 6, the initial closed loop step response of the aircraft may be viewed for roll response due to rudder deflection.

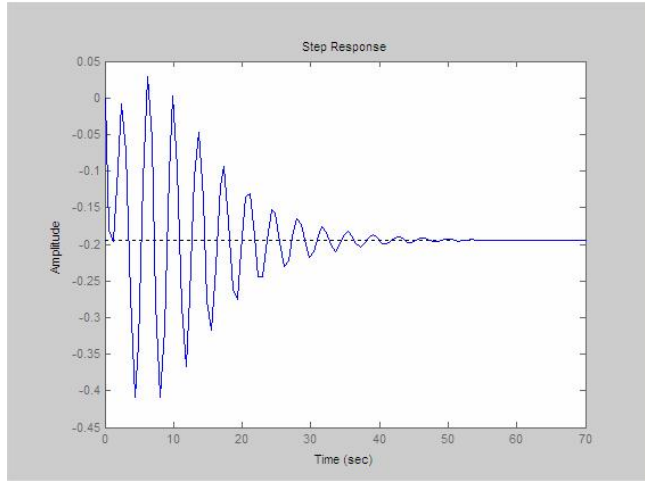


Figure 6. Step Response for Initial Closed Loop Aircraft Response for Roll due to Aileron Deflection

Aircraft response was analyzed for pitch, roll, and yaw characteristics, however, it was determined that the most significant response characteristics resulted from heading direction due to elevator deflection, roll response due to aileron deflection and pitch due to elevator deflection. The resultant longitudinal and lateral stability derivatives used to evaluate ARIES are located in Tables 1 and 2, respectively.

Longitudinal Stability Derivatives		
X_u	-0.7507	sec^{-1}
X_w	0.8232	sec^{-1}
Z_u	-1.8285	sec^{-1}
Z_w	-3.8995	sec^{-1}
$Z_{\dot{w}}$	-0.0294	rad^{-1}
Z_{α}	-137.55	ft/sec^2
$Z_{\dot{\alpha}}$	-1.0384	ft/sec
Z_q	-9.2685	ft/sec
$Z_{\delta e}$	-39.16	ft/sec^2
M_u	0.0000	$(\text{ft}\cdot\text{sec})^{-1}$
M_w	-0.1020	$(\text{ft}\cdot\text{sec})^{-1}$
$M_{\dot{w}}$	-0.0014	$(\text{ft})^{-1}$
M_{α}	-3.5967	sec^{-2}
$M_{\dot{\alpha}}$	-0.0495	sec^{-1}
M_q	-0.4414	sec^{-1}
$M_{\delta e}$	-1.8653	sec^{-2}

Table 1. Longitudinal Stability Derivatives for ARIES Aircraft.

Lateral Directional Derivatives		
Y_{β}	-26.75	ft/sec ²
Y_p	0.0000	ft/sec
Y_r	-2.5043	ft/sec
$Y_{\delta a}$	0	ft/sec ²
$Y_{\delta r}$	21.75	ft/sec ²
N_{β}	2.6450	sec ⁻²
N_p	-0.1114	sec ⁻¹
N_r	-0.2484	sec ⁻¹
$N_{\delta a}$	-0.0915	sec ⁻²
$N_{\delta r}$	-2.1567	sec ⁻²
L_{β}	-0.0934	sec ⁻²
L_p	-0.4399	sec ⁻¹
L_r	0.1660	sec ⁻¹
$L_{\delta a}$	0.7143	sec ⁻²
$L_{\delta r}$	0.0424	sec ⁻²

Table 2. Lateral Stability Derivatives for ARIES Aircraft

Dutch roll characteristics were found using an approximation corresponding to roll response due to aileron deflection. The spiral mode and roll mode were evaluated similarly using approximations. The spiral mode neglected aircraft response due to side forces and bank angle whereas the roll mode was estimated with respect to pitch rate. The short period and phugoid response characteristics for the aircraft were compared to MIL-F-8785C specifications in order to attempt to achieve Class 1 Level 1 characteristics. In comparing Dutch Roll Mode, Spiral Mode, Roll Mode, the Phugoid and Short Period Response for the aircraft with no compensation networks, the following results were obtained. Comparisons for results of the aircraft may be viewed in Table 3.

Unaltered Feedback Response			Military Specifications	
ω_{np}	1.297005838	rad/sec		rad/sec
ζ_p	0.289415714		>0.04	
$t_{1/2p}$	1.84	sec		sec
$N_{1/2p}$	0.38	cycles	-	cycles
ω_{nsp}	2.309040973	rad/sec		rad/sec
ζ_{sp}	0.95732352		$0.35 < \zeta_{sp} < 1.3$	
$t_{1/2sp}$	0.31			
$N_{1/2sp}$	0.11	cycles	-	cycles
ω_{nDR}	1.738992704	rad/sec	1	rad/sec
ζ_{DR}	0.540795329		0.19	
τ_{roll}	2.273199082	sec	1	sec
T_{spiral}	0.22	sec	12	sec

Table 3. Comparison of Unaltered Aircraft Characteristics to MILSPECS 8785C-Section 3

IV. Software Systems

A. Micropilot Horizon. The Horizon software was our means to communicate and command the Micropilot g2028 Autopilot System. It provided a user friendly point and click interface, and was easily integrated into our ground control system which ran on Windows XP operating system. Through Horizon we were able to monitor the autopilot, change waypoints in real time, upload new flight plans, initiate holding patterns and adjust feedback loop gains. To ensure a safe flight, Horizon allowed any flight plans to be simulated on the ground before actual flight. This prevented sending erratic flight patterns to the Micropilot system.

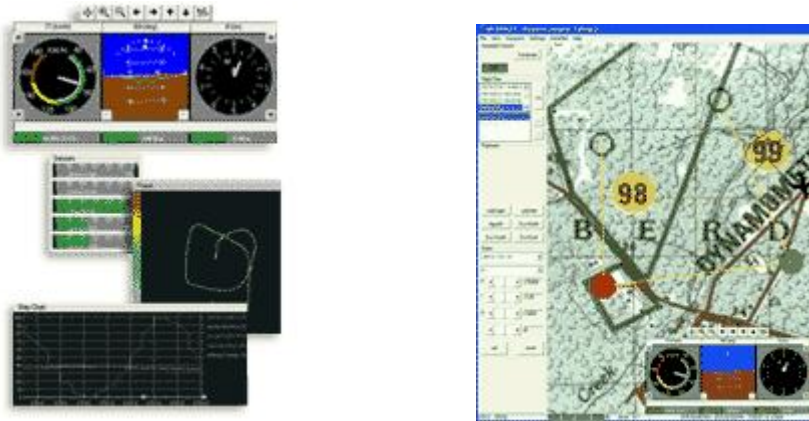


Figure 7. Micropilot Horizon Interface

B. Solidworks 2005. Solidworks 2005 was used to calculate mass properties, i.e. moments of inertia, location of center of gravity, weight of ARIES system. The Solidworks model without the Monokote coating is shown in Figure 8.

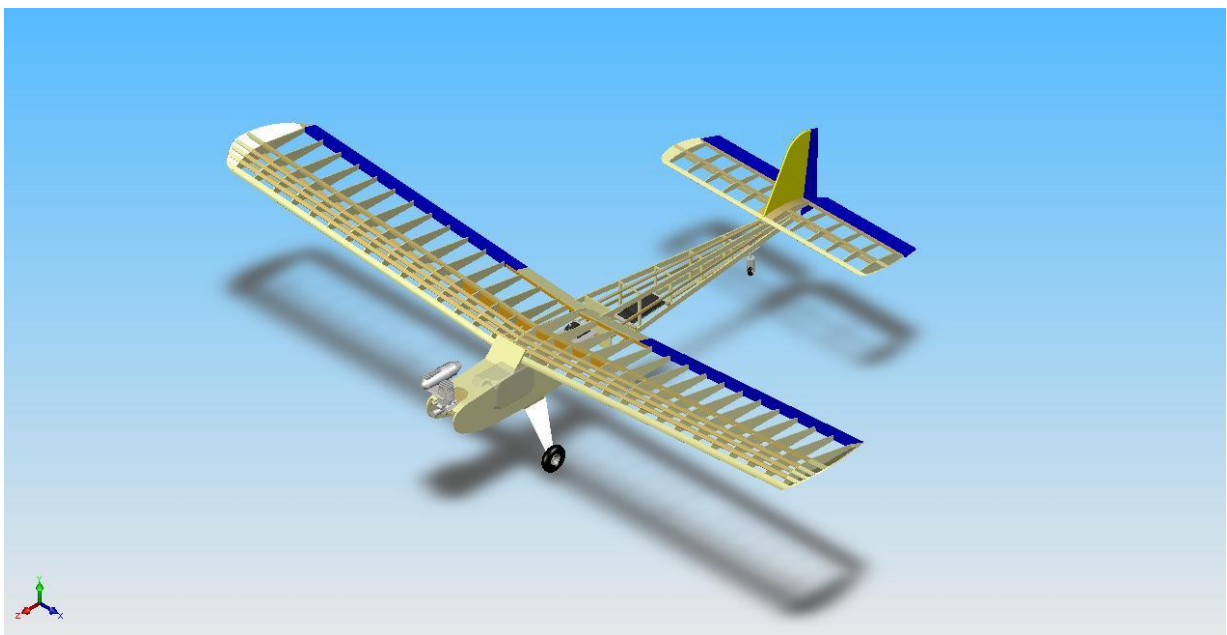


Figure 8. Solidworks Model of Senior Telemaster

V. Hardware System

A. **Micropilot g2028 Autopilot System.** In order to direct the control surfaces, the Micropilot MP2028^s provides the autonomous control. The Micropilot autopilot system provides control through a PID series loops. A PID feedback loop involves three gains denoted by P, I and D. P is for proportional, I for integral and D for differential. Proportional gain deals with the difference between actual and desired heading. Integral gain constitutes the sum of errors in the feedback loop. Differential gain deals with the error rate of change. For example, in order to control roll, Micropilot determines the necessary bank angle to reduce the divergence between the actual and desired heading. The importance of stability analysis was the determination of initial gain values used for flight test. The more precise the gain inputs are initially, the quicker the aircraft responds to changes. This was accomplished by trial and error involving flight-testing of ARIES.

The Micropilot microprocessor is an integrated circuit chip containing a servo board, a communication link, a GPS system, a pressure altimeter, a pitch rate gyro, a roll rate gyro, a yaw rate gyro, and an airspeed transducer. The servo board connects to the aircraft RC control unit to allow for manual override.



Figure 9. Micropilot g2028 Autopilot System

B. **Communication System.** The XStream-PKG 900 MHz Stand Alone Radio Modem was obtained from www.maxstream.net. The XStream-PKG-R 900 MHz stand-alone RF Modem provides long range (up to 7 miles) in a low cost wireless solution. The range requirement was the most important requirement concerning a modem purchase. The modem is coupled with a DIP-switchable RS-232/422/485 interface board and resides in an anodized aluminum enclosure.



Figure 10. XStream-PKG 900MHz Stand Alone Radio Modem.

Performance

Indoor/urban Range w/ 2.1 dB dipole antenna	up to 1500' (450 m)
Outdoor line-of-sight Range w/ 2.1 dB dipole antenna	up to 7 miles (11 km)
Receiver Sensitivity	-110 dBm (@9600 bps)
Outdoor line-of-sight Range w/ high-gain antenna	up to 20 miles (32 km)
Transmit Power output	100 mW (20dBm)
Receiver Sensitivity	-110 dBm (@9,600 bps Throughput Data Rate), -107 dBm (@19,200 bps)
Interface Data Rate	10 - 57600 bps (including non-standard baud rates)
Throughput Data Rate	9,600 or 19,200 bps
RF Data Rate	10,000 bps (@9,600 bps Throughput Data Rate) or 20,000 bps (@19,200 bps)

Power Requirement

Power Supply Voltage	7-18 V
Transmit Current	200 mA
Receive Current	70 mA
Power Down Current	<1 mA

C. Imagery System. The wireless color camera system with 2.4 GHz was obtained from www.helihobby.com. The complete package comes with the CCD Wireless camera, on board transmitter, ground receiver, microphone system, and cables mounting accessories. The size of the camera is 0.79 inches in height and 1.2 inches in length. The receiver is an A/V type of 4 channels option. The camera and receiver are located at the center of the fuselage to minimize vibration from the engine. The aerial imagery received from the airplane will be sent to the ground control system.



Figure 11a. Wireless Color Camera System



Figure 11b. Wireless Color Camera

D. Power System. The power system consisted of two independent rechargeable battery supplies. The first system consisted of 4 AA Ni-Mh Energizer rechargeable batteries which provided 5.2VDC to the servos. The batteries were rated at 2300 mAh, which permitted an hour's worth of use by the servos. The second system consisted of 8 AA Ni-Mh Energizer rechargeable batteries which provided 11.6VDC for the Micropilot system, the video color camera and the Xstream standalone radio modem. The batteries were rated at 2500mAh.

Acknowledgments

We the Cal Poly Pomona ARIES team would like to acknowledge Northrop Grumman especially Mr. Barnaby Wainfan, Dr. Donald Edberg of Cal Poly Pomona Aerospace Engineering Department, Micropilot Inc., Cal Poly Pomona Design Build Fly Team, Mr. Francisco Ccasa of F.C. Machining, and Cal Poly Pomona Mechanical Engineering Department.

References

¹*MP2028g Installation and Operation Manual*, © 1998-2005, MicroPilot Inc. Stony Mountain, MB, Canada.

²*HORIZON^{MP} User's Guide*, © 1998-2004, MicroPilot Inc. Stony Mountain, MB, Canada.

³Nelson, Robert C., *Flight Stability and Automatic Control*, McGraw-Hill, New York, 1989.

⁴Solidworks 2005, Software Package, Ver. 2005 SP0.0, 1995-2004 Solidworks Corp.

⁵*HORIZON^{MP}*, Software Package, Ver. 3.0.54, 1998-2004, Stony Mountain, MB, Canada.